Experimental models for Murray's Law

Dai Akita[1,2], Itsuki Kunita[3], Mark D. Fricker[4], Shigeru Kuroda[2], Katsuhiko Sato[2], Toshiyuki Nakagaki[2*]
[1] *Graduate School of Life Science, Hokkaido University, N10 W8, Sapporo, Japan*
[2] *Mathematical and Physical Ethology Laboratory, Research Center of Mathematics for Social Creativity, Research Institute for Electronic Science, Hokkaido University, N20 W10, Sapporo, Japan*
[3] *International Research Center for Medical Sciences, Kumamoto University, 2-2-1 Honjo, Chuo-ku, Kumamoto, Japan*
[4] *Department of Plant Science, University of Oxford, Oxford, OX1 3RB, UK*

(Dated: November 2, 2016)

Transport networks are ubiquitous in multicellular organisms and include leaf veins, fungal mycelia and blood vessels. While transport of materials and signals through the network plays a crucial role in maintaining the living system, the transport capacity of the network can best be understood in terms of hydrodynamics. We report here that plasmodium from the large, single-celled amoeboid *Physarum* is able to construct a hydrodynamically optimized vein-network when evacuating biomass from confined arenas of various shapes through a narrow exit. Increasingly thick veins developed towards the exit, and the network spanned the arena via repetitive bifurcations to give a branching tree. The Hausdorff distance from all parts of the plasmodium to the vein network was kept low, whilst the hydrodynamic conductivity from distal parts of the network to the exit was equivalent, irrespective of the arena shape. This combination of spatial patterning and differential vein thickening served to evacuate biomass at an equivalent rate across the entire arena. The scaling relationship at the vein branches was determined experimentally to be 2.53-3.29, consistent with predictions from Murray's law. Furthermore, we show that mathematical models for self-organised, adaptive transport in *Physarum* simulate the experimental network organisation well if the scaling coefficient of the current-reinforcement rule is set to 3. In simulations, this resulted in rapid development of an optimal network that minimised the combined volume and frictional energy in comparison with other scaling coefficients. This would predict that the boundary shear forces within each vein are constant throughout the network, and would be consistent with a feedback mechanism based on a sensing a threshold shear at the vein wall.

PACS numbers: 87.10.Ed, 87.17.Pq, 89.40.Cc, 89.75.Hc
Keywords: Slime mold, Transport network, Self-organization, Scaling law, Current-reinforcement, Hydrodynamics, Energy minimization

I. INTRODUCTION

Biological transport networks form part of the critical infrastructure that is required to distribute resources and information rapidly and efficiently throughout the entire body of a multicellular organism. They include the vascular systems of plants and animals and gastrovascular system of hydractiniid hydroids that are embedded within the organism, and the plasmodial veins of slime molds and the mycelial cords of fungi that effectively constitute the entire organism apart from the reproductive structures. These networks play a key role in the organization of the overall body plan, and the vessel size and network architecture are thought to follow quarter-power allometric scaling laws that relate the notional space-filling fractal branching pattern of the network to body size and metabolic rate according to metabolic scaling theory (MST) [1], or reflect the design of optimal transport networks [2–4].

In each case, the network comprises tubular elements with varying thickness and length, that are organised as a hierarchical branching tree, but may also contain a significant number of additional loops to improve performance under fluctuating loads or in the presence of damage [5, 6]. Whilst the vessel geometry clearly has an impact on the local fluid flow, the overall transport behaviour and scaling relationships are properties of the entire network. Unfortunately, however, most biological networks develop over extended time periods, cannot be characterised easily in their entirety, and are not amenable to manipulation or repetition, making it difficult to experimentally evaluate competing theories of network organisation and scaling exponents against empirical data.

Recently, attention has focussed on the acellular slime mold, *Physarum polycephalum* as a tractable model or-

*Corresponding author; e-mail nakagaki@es.hokudai.ac.jp

ganism to study the iterative interplay between structure and function in a self-organised biological transport network, and to help to determine the rules that may govern adaptive network development [7–15]. *Physarum* is a giant, single-celled amoeboid organism that grows rapidly as an extensive plasmodial network over the available space within a few hours as it forages for food. If resources are not located, it can also retract the plasmodium and redeploy the biomass elsewhere to support further foraging.

Here we exploit this latter behaviour to examine network formation during evacuation of the plasmodium from a set of arenas with varying geometric shape. Within a few hours, an intricate network develops within the initially uniform plasmodial sheet, that then serves to progressively transport biomass out of the arena via the single exit point. As the entire system is accessible, we can determine quantitatively: (i) the dimensions of the individual veins; (ii) the structure of the network that they form, including the space filling properties; (iii) how these contribute to the rate of biomass retrieval over the entire arena; (iv) whether the network that forms follows predicted scaling relationships at the vein junctions; and (v) how these parameters vary as the network adapts to different arena geometry.

In addition, a number of bioinspired mathematical models already exist that describe amoeboid movement, peristaltic waves and network formation in *Physarum* [8, 14–22]. In the case of network formation, current-reinforcement models [7, 8, 14] capture the behaviour of the biological system well, but so far none have been explicitly parametised from experimental results. These current reinforcement models include a non-linear current-reinforcement term that reflects the propensity of a tube to increase in diameter in response to the internal flow rate through the tube itself. Conversely, if the flow is too small the tube disappears at a rate determined by the decay term. By following the time-evolution of evacuation network formation, we can begin to link the experimental observations with appropriate values for the coefficients in the model.

In particular, we have examined whether the branching rule, originally proposed by Murray to describe the branching of arteries [23], holds for vein networks in *Physarum*, and would therefore provide theoretical support for the value of the current-reinforcement coefficient. Murray proposed that the relationship:

$$r_0^3 = r_1^3 + r_2^3 + \cdots r_n^3, \tag{1}$$

where r_0 is the radius of parent vein and $r_1, r_2, ...r_n$ are those of daughter veins, provides an optimal solution to balance the effect of reducing viscous drag with the cost of increasing vessel volume, assuming Hagen-Poiseuille flow. Murray's law has been validated by measurements of artery branching relationships for small vessels, that typically give an exponent ranging from 2.7 to 3.0 [24], and is often incorporated in predictions of network performance as a transition between area-preserving (r^2) for branching in large vessels to r^3 for branches closer to the terminal transport vessels (e.g., [1, 4]). Nevertheless, many of the assumptions underpinning these universal theories lack strong experimental support and are the subject of ongoing debate (e.g., [25]). Indeed, recent automated non-invasive measurements of vessel properties in vascular networks have been used to explicitly test different predictions for the scaling exponents from several theoretical models. The authors concluded that none of the current methods provides a good description of real vascular networks, and they advocated the development of new relationships between vessel geometry and global network properties [26]. It is therefore important to link experimental measurements of vessel properties, with theoretical principles, such as Murray's Law, that govern idealised network behaviour, when constructing predictive models of network organisation and performance in *Physarum*. Even so, we have made simplifying assumptions, most notably that the time-scale for network formation (hours) allows us to neglect the complex viscoelastic properties of the plasmodial body and contraction-relaxation based shuttle streaming (min). Instead, we treat the plasmodial veins as rigid cylindrical pipes in each time step, but with the capacity to change average radius in response to fluid flow in the next time step.

II. MATERIALS AND METHODS

A. Establishment of an evacuation network from a confined space

Plasmodia of *Physarum polycephalum* were grown on 1% (w/v) agar (S-7, Ina Food Industry) with oat meal flakes (Quaker) in the dark.

Protoplasmic sheets were obtained by excision of tissue from thick veins of actively growing plasmodium, and sandwiching it between glass plates with a gap 0.12∼0.17 mm. Within a few seconds, the protoplasm gelled to give a uniform sheet. The sheet was transferred to a small arena cut out from plastic film, and placed on agar (See panels `init` and `0h` in Fig.1). Food was placed on the exit to encourage the slime mold to evacuate the arena and promote formation of the vein network. A range of arenas with different shapes were tested including circular (C, 10 mm diameter), rectangular (R1, 6 mm × 17.5 mm; R2, 7.5 mm × 14.5 mm; R3, 10 mm × 10 mm; R4, 14 mm × 7.3 mm; R5, 20 mm × 5 mm), or irregular (A).

Time-lapse images were obtained with transmitted light. The thickness was estimated as $h = -\log(I/I_0)$ according to the Beer-Lambert law, where I and I_0 were the intensities of transmitted and incident light. The network morphology was obtained by manually tracing the main veins on the 2-dimensional map of h. Experiments were repeated five times for the circular and rectangular shapes, and three times for the irregular shape. To analyze the time-course of changes in h, the map of h was

processed initially with a averaging filter of radius 350 μm to give h_{av}. From the locally averaged thickness h_{av}, we estimated the evacuation time-constant τ and the initial value h_0 of $h_{\mathrm{av}} = h_0 \exp(-t/\tau)$ for each pixel so that the squared error was minimized.

B. Quantitative analysis of the network organisation and transport capacity

The space-filling properties of the network were estimated from the maximum distance between every pixel in the arena and the nearest pixel on the manually extracted network of thick veins to give the Hausdorff distance. Mathematically, the Hausdorff distance between two subsets A and B of a metric space (X, d) is defined as

$$d_H(A,B) = \max\{\sup_{x\in A}\inf_{y\in B} d(x,y), \sup_{y\in B}\inf_{x\in A} d(x,y)\}.$$

Given that A is the arena and B is the traced network,

$$\sup_{y\in B}\inf_{x\in A} d(x,y) = 0$$

because $B \subset A$. It follows that

$$d_H(A,B) = \sup_{x\in A}\inf_{y\in B} d(x,y),$$

where $d_H(A,B)$ represents the maximum distance between every pixel in the arena and the nearest pixel on the network. To compare results between the different arena shapes, the Hausdorff distance was divided by the maximum distance within the arena to give the normalized Hausdorff distance.

The predicted performance of the network was estimated from the hydraulic conductivity of each vein. Assuming Hagen-Poiseuille flow, the flow rate Q in a vein with a pressure difference ΔP is:

$$Q = \frac{\pi r^4}{8\nu L}\Delta P, \tag{2}$$

where r and L are the radius and the length of the vein, respectively, and ν denotes the viscosity.

The conductivity $\pi r^4/8\nu L$ was estimated from manual measurements of the thickness and length of each vein segment, and summed to give the hydrodynamic conductivity (HC) for any point in the network to the exit point.

C. Validation methods for Murray's law

To determine the relationship between the radii of veins at a junction, 57 nodes were measured from the set of circular networks. r_0 was defined as the maximum radius out of the 3 veins at the branch and r_1 and r_2 the daughter radii. The exponent n was then calculated to satisfy the relationship $r_0^n = r_1^n + r_2^n$ for each junction.

Note that errors in radii cause an asymmetric error in the exponent n by this calculation, and thus the mean of the calculated exponent across all junctions is not appropriate for the estimation of the overall scaling coefficient, n. For example, given that the measurement of r_0 gives a value of an interval $[r_0-\delta, r_0+\delta]$ and the error propagates to the calculated exponent as an interval $[n-\delta_1, n+\delta_2]$, where $\delta_1 \neq \delta_2$, this leads to asymmetry of the distribution of the exponent. Thus, to estimate the exponent n fairly, we transformed n to give a normal distribution using the arctan transformation proposed by Suwa *et al.* from similar studies on arteries [27], and then calculated the interval range for n from the inverse transformation of the arctan confidence intervals.

III. RESULTS

A. Evacuation networks form rapidly and remain topologically stable

Plasmodial sheets of *Physarum* placed in a constrained arena rapidly expanded to fill the available space to give a near uniform thickness (Fig. 1, 0-1h). The introduction of a food resource at the exit stimulated evacuation of the slime mold from the arena through an emerging network of veins that ramified throughout the arena (Fig. 1, 2-9h). Once the initial network of thicker veins was visible, the topology remained stable throughout the evacuation period. The flux of protoplasm flowing through the branching network and thence out the arena was apparent from the almost uniform reduction in thickness of the plasmodium, until about 10h when the thinnest parts become resolved as a very fine network (Fig. 1, 10-14h). Similar observations were made on all replicates for each different shape of arena (n=5 for the circular and the rectangular shapes, n=3 for the irregular shape).

B. Evacuation kinetics through the vein network are similar across entire space, and independent of arena shape

The near uniform reduction in thickness observed across the arena, implied that the rate of protoplasm removal was similar for all parts of the system irrespective of the distance to the exit. To quantify the rate of removal, the locally averaged change in cell thickness was measured from inter-vein regions adjacent to the exit (Fig. 2, A), mid-way away (Fig. 2, B), and nearly opposite the exit (Fig. 2, C). Although the euclidean distance to the exit point varied by a factor of four, the rate of protoplasmic removal was almost identical and seemed to decrease exponentially. We therefore calculated the best-fit exponential to the time-series for each pixel and mapped the half-time parameter of the decay across the

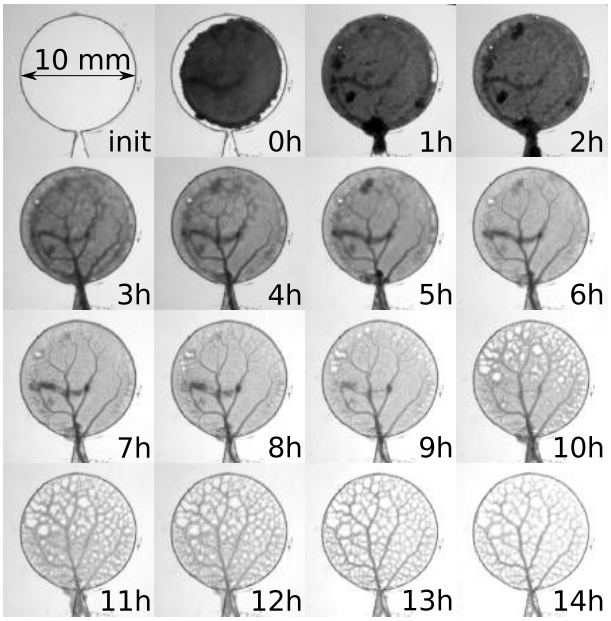

FIG. 1: Time course images following the development of a veination network by *Physarum* during evacuation from a confined circular arena.

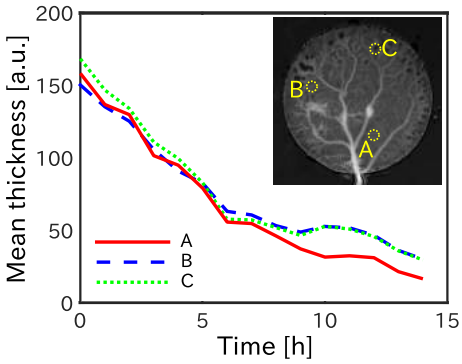

FIG. 2: Changes in the thickness of the plasmodium over time, monitored at three different inter-vein regions. Each lines mean the change of the thickness index averaged in the circle.

whole arena (Fig. 3, d). The colour-coded map of the time-constant shows a consistent value of 6-7 hour in the inter-vein regions (Fig. 3, d).

To determine whether this organised behaviour was a consequence of using a circular arena or represented a general adaptive property of the network to achieve efficient protoplasmic movement and redeployment, time-constant maps for rectangular arenas that differed in aspect ratio, and an arena with a more complex shape were calculated in a similar manner. As Fig. 3 (e) and (f) show, the inter-vein regions of rectangular and irregular shapes have remarkably consistent time-constants of around 8 hour and 15 hour, respectively, for the inter-

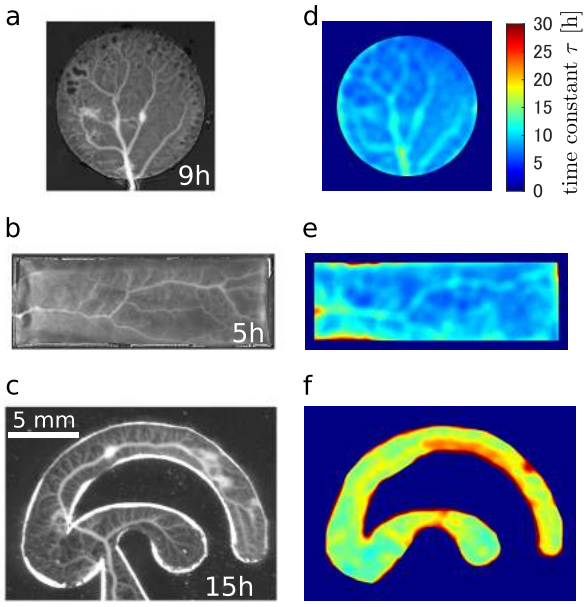

FIG. 3: Thickness images and those time-constant maps. (a, b, c): thickness images at a time for circular, rectangular, and irregular shape. (d, e, f): maps of time-constant by which thickness decrease exponentially. The scale bar is applied to all the images, and the colour bar is applied to d, e, and f.

vein regions. That is, the kinetics of evacuation are almost identical across the whole arena, irrespective of the arena shape.

We infer from these results that the spatial disposition of the vein network that emerges during network formation, and the variation in thickness combine to service all regions of any shaped arena equally well.

C. Evacuation networks cover space effectively

To quantify how well the vein network serviced the entire space, the maximum distance from any point in the arena to the vein network was calculated as the normalised Hausdorff distance for each arena shape. Values were uniformly small in comparison to the extent of the available space, ranging from 0.1 to 0.2 (Fig. 4). This means that the main veins were distributed almost uniformly over the arena so that there were no isolated regions far from any vein.

D. Variation in network vein thickness gives similar hydrodynamic conductivity with distance

Whilst movement of material to the veins is reflected in the normalised Hausdorff distance, movement within the network depends on the thickness and hierarchical branching pattern of the vein segments, and the pres-

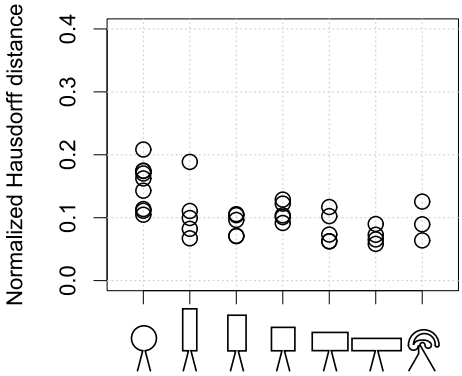

FIG. 4: Normalized Hausdorff distance for networks formed in each arena shape. The shapes tested are illustrated along the abscissa: from left to right, circle, tall rectangles, square, wide rectangles, and an irregular shape. The exit is located at the bottom of shapes, indicated by the trapezoid channel. (n=5 for the circular and the rectangular shapes, n=3 for the irregular shape).

sure gradients driving flow. Thus, flow from any point in the network to the exit is governed by the hydrodynamic conductivity (HC) of the pathway to the exit, which can be estimated from the physical dimensions of the veins themselves, and any variation in the actin-myosin contraction system present throughout the plasmodium. Interestingly, the measured hydrodynamic conductivity was similar for peripheral points in the network (Fig. 5), and varied much less than the physical distance to the exit with position in the arena. The HC contours match the different arena shapes and help to explain the constant evacuation rate.

E. Examination of Murray's law on the thickness relationship before and after a bifurcation

We infer from the consistency of the measured hydrodynamic conductivity that the branching pattern and parent-daughter vein thickness ratio at each bifurcation junction were likely to conform to a scaling relationship. In other transport systems dominated by viscous drag, Murray's Law predicts a cubic exponent according to Eq. (1), whilst networks with larger vessels follow an area preserving relationship (i.e. r^2). The scaling exponent was therefore calculated for the 57 three-way junctions present in the networks grown in the circular arenas (Fig. 6, left). The initial distribution was highly skewed with the median 3.15, but was normalised using an arctan tranformation (Fig. 6, right), as used by Suwa *et al.* [27] for blood vessel networks. The correlation coefficient between $\arctan n$ and r_0 was 0.015 and the mean and 95% confidence interval were 1.235 ± 0.045. This gave an estimate of n from the tangent of the interval as between 2.53 to 3.29, which appears to be reasonably consistent with the expectation of $n \sim 3$ from Murray's

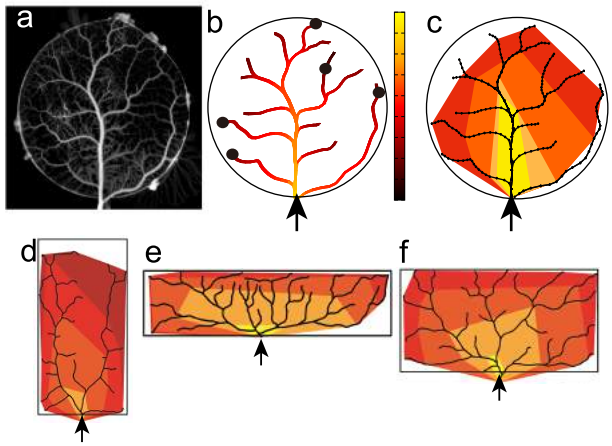

FIG. 5: Hydrodynamic conductivity of vein-network observed in the confined circular shape. (a) Thickness image of vein-network in the circle with diameter 1 cm. (b) Hydrodynamic conductivity along the main vein-network. A certain value of same HC was marked by the black dots on the network near the boundary of confined space. (c) Convex envelop for the dots marked in the figure b. (d, e, f) The same analysis on other shapes. Arrows indicate the location of exit.

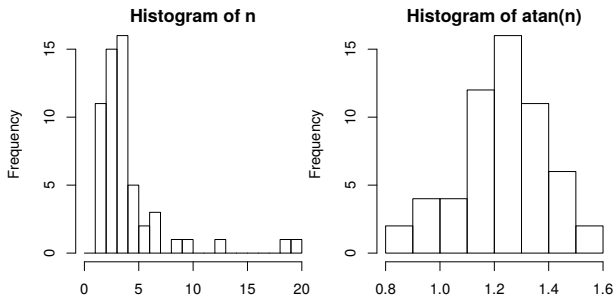

FIG. 6: Histogram showing the distribution of the vessel scaling exponent n calculated from $r_0^n = r_1^n + r_2^n$ for all bifurcations in the set of circular evacuation networks. The $\arctan(n)$ transformation normalised the data and gives a mean $\pm$ S.D. of 1.235 ± 0.045

law. Nevertheless, we do not have a good understanding of the extreme values of n in the measured distribution.

IV. EXPLORING THE CONSEQUENCES OF SCALING EXPONENTS IN MATHEMATICAL MODELS OF NETWORK FORMATION WITH CURRENT-REINFORCEMENT DYNAMICS

A. Outline of the standard current reinforcement model

The standard biologically-inspired mathematical model for adaptive network formation proposed by Tero *et al.* [8] has successfully reproduced a number of key experimental results describing the behaviour of

Physarum (e.g., [9–11], although none of the parameters in the simulations were explicitly based on experimental measurements. In the model the plasmodium is represented by a random meshwork of tubular channels that are assumed to be rigid and cylindrical in each time step as a simplifying assumption that neglects their more complex viscoelastic properties.

Vertices i and j are connected by channel ij, with uniform diameter r_{ij}, length L_{ij}, and flow rate Q_{ij}. Volume conservation is assumed at vertex i as

$$\sum_j Q_{ij} = Q_0, \tag{3}$$

where Q_0 is a nonzero constant if vertex i is a source or sink of current, and Q_0 is zero otherwise.

If the current sources and sinks with Q_0 are given, and L_{ij} and r_{ij} of all channels are known, all Q_{ij} can be determined. Once there is flow on the network, the current-reinforcement rules modify the thickness of each channel in the next time step according to the flow it is carrying.

Using the notation of Eq. (2),

$$Q_{ij} = \frac{D_{ij}}{L_{ij}} \Delta P_{ij}. \tag{4}$$

the conductivity per length, $D_{ij} = \pi r^4/8\nu$, evolves over time in response to the flow,

$$\frac{\mathrm{d}D_{ij}}{\mathrm{d}t} = f(|Q_{ij}|) - D_{ij}, \tag{5}$$

where f is a monotonically increasing continuous function satisfying $f(0) = 0$, and we assume that L_{ij} does not change.

Eq. (5) contains two antagonistic components: $f(|Q_{ij}|)$ represents a thickening factor that increases with the current, whilst $-D_{ij}$ is a intrinsic thinning factor. Thus, the thickening component dominates for a channel with a larger current, and the thinning effect dominates for one with smaller current at each time step. The complete temporal evolution of the network is then calculated iteratively with the updated conductivities.

In the numerical simulation described here, we set $f(|Q_{ij}|) = |Q_{ij}|^\mu$, where μ is a positive parameter as Tero *et al.* originally assumed [8]. Considering the equilibrium state as $\mathrm{d}D_{ij}/\mathrm{d}t = 0$, we see that

$$|Q_{ij}|^\mu = D_{ij} \propto r^4, \tag{6}$$

which means $|Q_{ij}| \propto r^{4/\mu}$. Therefore, using the notation of III E, we can express the exponent rule as

$$r_0^{4/\mu} = r_1^{4/\mu} + r_2^{4/\mu} \tag{7}$$

and see the correspondence $n = 4/\mu$. To satisfy Murray's law exactly μ must be 4/3, but it is instructive to examine other values of the exponent as well. Indeed, in previous simulations we have employed a different functional form for f, namely:

$$f(|Q_{ij}|) = \frac{|Q_{ij}|^\gamma}{(1 + |Q_{ij}|^\gamma)} \tag{8}$$

which tends to 1 in the limit for high flux, equivalent to $\mu = 4/4$, but we have not previously explored the regime where Murray's Law ($\mu = 4/3, n = 3$) or area-preserving rules ($\mu = 4/2, n = 2$) might apply.

B. Numerical simulation of the model

Virtual arenas were constructed to match the shapes used in the experiment with a scale 10 μm/px, and a random mesh, generated by a Delaunay triangulation with random vertices giving density of 1/500 px^{-2} within the arena shape. A single vertex at the exit was designated as a sink, whilst all others were set as sources with an initial current of 0.1. The radii r of all veins were set to be 0.1 initially, and the conductivity was equal to r^4. Simulations were run with a short initial time step ($\Delta t = 0.001$) over the period $t = 0$ to $t = 0.1$, followed by $\Delta t = 0.01$ for $t = 0.11$ to $t = 1$, and $\Delta t = 0.1$ for $t = 1.1$ to $t = 50$. Note that we did not attempt to model the change in thickness of the rest of the plasmodial sheet, which might be represented as variation of the input current to each node over time, as the purpose of the simulation was to capture the initial development of the evacuation network.

The simulation reached a steady state as the time development. Figure 7 shows the network morphology of the final state with parameters $\mu = 4/2, 4/3, 4/4$ and $4/5$, that correspond to the exponents $n = 2, 3, 4$ and 5.

When μ was greater than 1 ($\mu = 4/2$ and $4/3$), a subset of the available veins thickened and formed a branching tree from the exit site with progressively thinner veins through repetitive bifurcations towards the boundary of the arena. When μ was 1 ($\mu = 4/4$), the branching tree contained additional loops, whilst when μ was less than one ($\mu = 4/5$), the vein thicknesses were more homogeneous and there were many loops. Visual inspection suggested that $\mu = 4/3$ and $4/2$ most closely resembled the experimental data.

To compare the simulated networks quantitatively with the experimental network, the normalised Hausdorff distance was calculated for the main network, defined as the set of veins containing the top 10% of the thickest veins (Fig. 8). This limit was selected to contain the minimum radii in the simulation that could be measured in the experimental networks. Using this criterion, the normalised Hausdorff distance was small across all arena shapes, and similar to the values observed for the experimental systems, particularly for $\mu = 4/2$ and $4/3$. Likewise, the hydrodynamic conductivity was similar to the experimental networks for $\mu = 4/2$ and $4/3$, with points near the boundary showing similar conductivity. We infer that the current-reinforcement simulation model can

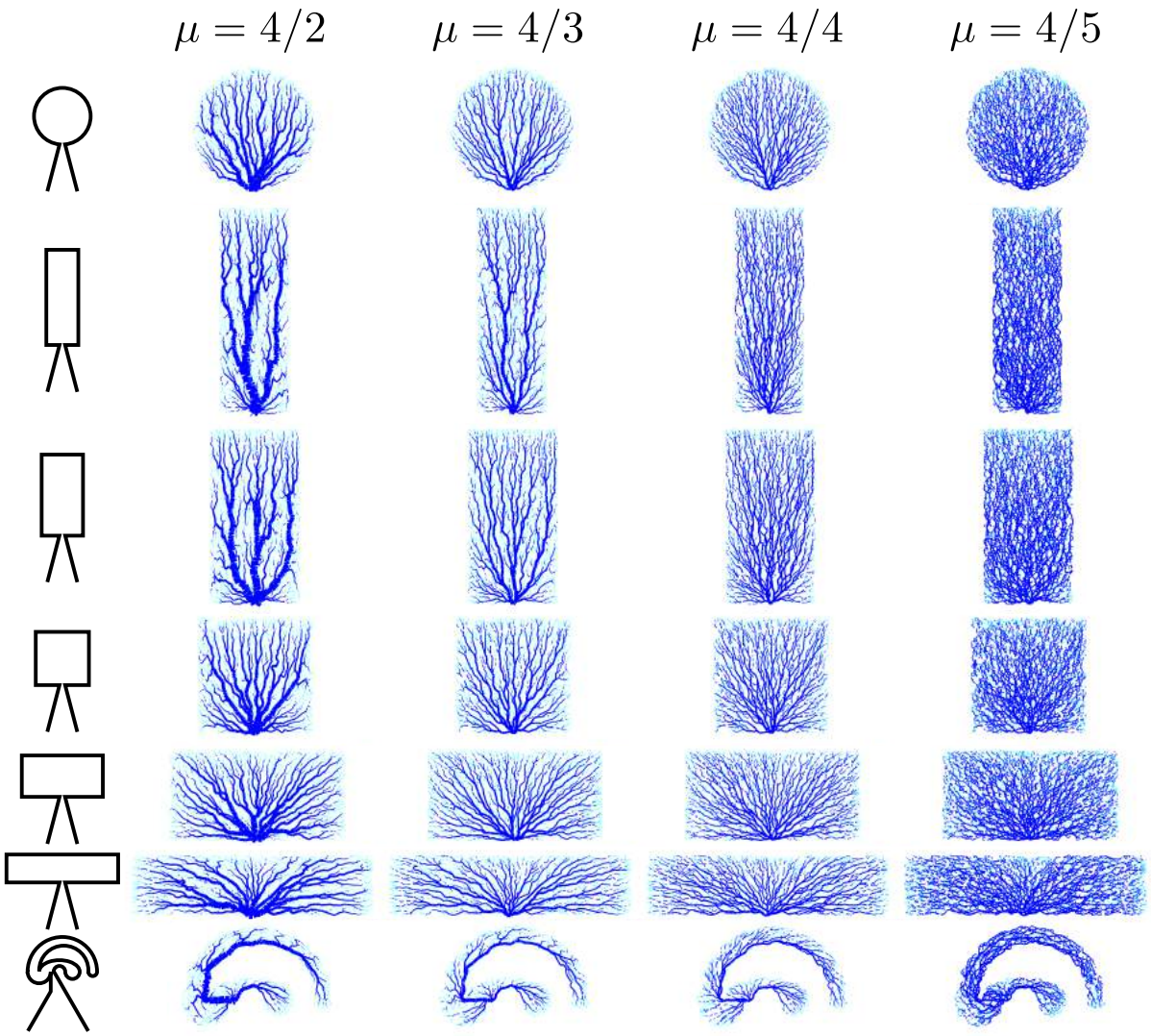

FIG. 7: Simulation results for varying μ in the different arena shapes. The main veins are drawn with radius proportional to the simulation result, whilst the very thin veins are drawn with dashed, dotted, or light blue line.

reproduce the basic characteristics of the experimental *Physarum* networks when $\mu = 4/2 \sim 4/3$.

C. Impact of μ on network volume and viscous drag

The theoretical derivation for the r^3 exponent in Murray's Law was based on balancing the energy required to overcome viscous drag forces with the cost of maintaining the volume of the network [23]. It is therefore instructive to examine the time-evolution of these two parameters and their dependence on μ in the simulation model as the system tends towards steady-state.

The change in the energy required for transport over time for simulations of the circular arena is shown in Fig. 9, where the total frictional energy was calculated as:

$$E = \sum_{i \in \text{veins}} \Delta P_i Q_i = \sum_{i \in \text{veins}} \frac{L_i Q_i^2}{D_i}. \tag{9}$$

During the initial stages of the simulation the frictional energy decreased rapidly as the network shifted from the random network of tubes with homogeneous low diameter, to the branching tree morphology (Fig. 9, top). The minimum energy dissipation was achieved with $\mu = 4/2$. Nevertheless, the time course was not quite monotonic, with a slow increase observed after the minimum value was reached around t=25 (Fig. 9, top), consistent with the contribution of other factors in the cost function.

The total volume of the tubular veins, representing the energy cost to maintain the network [23], was calculated

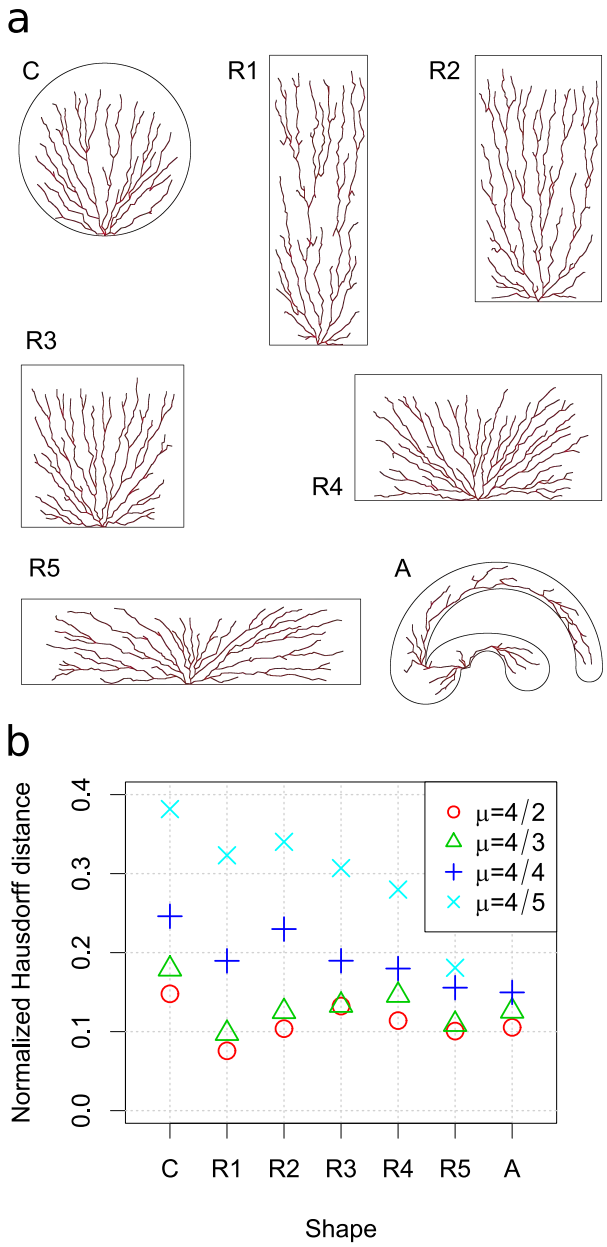

FIG. 8: Analysis of main network from the simulation model, comprising the top 10% of the thickest veins. (a) The main networks for $\mu = 4/3$. (b) Normalized Hausdorff distance between the main network and all points in the arena.

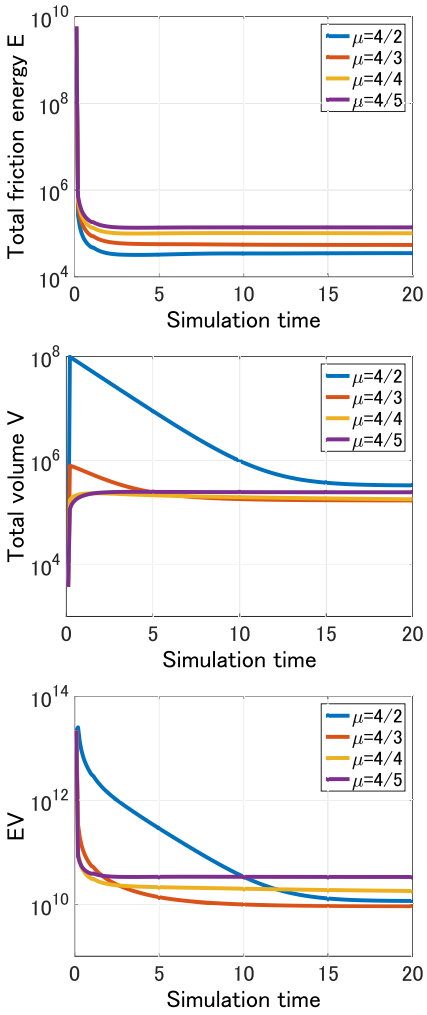

FIG. 9: Time courses for the change in frictional energy E (top), total volume V (middle), and their product EV (bottom) for the simulation results from the circlular arena.

as:

$$V = \sum_{i \in \text{veins}} \frac{\pi r_i^2 L_i}{2}, \tag{10}$$

The total volume of the network increased in the very early phase of the numerical simulation, particularly in the case of $\mu = 4/2$, and to a lesser extend $\mu = 4/3$. This pronounced surge was caused by setting the initial tube radii to be small (0.1) and equal to mimic the emergence of the tubular network from a uniform sheet. The total volume of the network then gradually declined to a steady state value by the end of the simulation (Fig. 9, middle). In the steady state, the lowest network volume was realised with $\mu = 4/3$ (Fig. 9, middle).

Following expectations from Murray's Law, we examined the combination ($E \times V$) of the friction energy and the total volume (see Fig. 9, bottom). The steady state value of $E \times V$ was the lowest for $\mu = 4/3$, and the minimum was realized in a relatively early phase of time course.

Taken together, it appears that (i) self-organised network formation in *Physarum* conforms to a scaling coefficient of $\mu = 4/3$ in experimental results; (ii) when the same 4/3 scaling is used in the biologically-inspired current-reinforcement model, it simulates the overall characteristics of the real network; and (iii) the model minimises the combination of network volume and frictional energy.

V. DISCUSSION

The plasmodium of the slime mold *Physarum polycephalum* spontaneously creates complex networks that provide an accessible model for the development of self-organised adaptive transport systems. It is capable of solving path-finding problems [10, 11], and can realise reasonable solutions to complex spatial network tasks designed to mimic human infrastructure networks. For example, Tero *et al.* [9] showed that the vein network constructed by *Physarum* on agar constrained to the Kanto region of Japan was comparable to the real JR railway network in terms of transport efficiency and resilience. In a similar manner, Adamatzky and Jones have compared road networks in the UK, USA, and Germany with those made by *Physarum* [28, 29]. In parallel, a number of models have emerged that capture the behaviour of *Physarum* using current-reinforcement rules where the flow modifies the network architecture, which in turn modifies the flows.

Nevertheless, the models have not so far been parametrised directly from the experimental data, nor have the functional form of the feedback terms been linked to theoretical expectations from fluid flow dynamics. Thus in this paper, we have first measured the development of an evacuation network as *Physarum* exits a bounded arena to determine whether the network geometry follows expectations from fluid dynamics and energy minimisation criteria developed by Murray [23], and second examined the consequence of running the current-reinforcement model with the experimentally-validated 4/3 scaling coefficient. The results provide evidence that *Physarum* does conform to the cost balance behaviour proposed by Murray and that simulations run with this parameter provide comparable solutions, whilst minimising the combination of shear stress and vessel volume. It is possible that the fit to the data could be improved with more precise measurement of the actual cross-sectional area available for flow within the tube, rather than our manual estimate from the external tube diameter, assuming there is an almost linear relationship between internal and external diameter [30]. Nevertheless, to our knowledge, this is the first time that experimental network formation, network theory and network simulation have all converged to give consistent results in a model system.

Interestingly, as the *Physarum* network appears to follow the exponent scaling predicted by Murray's Law, we can also make predictions concerning the wall shear stress throughout the network. The shear stress $\tau(r_0)$ at the wall caused by Hagen-Poiseuille flow in a cylindrical tube (radius r_0) is given by

$$\tau(r_0) = -\eta \left.\frac{\partial v}{\partial r}\right|_{r=r_0} = -\frac{r_0}{2}\frac{dp}{dx} \tag{11}$$

from the velocity profile

$$v(r) = \frac{1}{4\eta}\left(r_0^2 - r^2\right)\frac{dp}{dx} \tag{12}$$

where r is distance from the center axis of cylinder to periphery, and x is distance along the center axis from the end of cylinder. Substituting $Q = (\pi r_0^4/8\eta)(dp/dx)$ into the above shear stress formula, we obtain

$$Q = \frac{\tau(r_0)\pi r_0^3}{4\eta}. \tag{13}$$

Combining this and the mass conservation around the bifurcation point of vein $Q_0 = Q_1 + Q_2$, we find

$$\tau(r_0)r_0^3 = \tau(r_1)r_1^3 + \tau(r_2)r_2^3 \tag{14}$$

where r_1 and r_2 are radii of two daughter veins [23].

As the experimental results confirm $r_0^3 = r_1^3 + r_2^3$, we infer that $\tau(r_0)$, $\tau(r_1)$ and $\tau(r_2)$ are equal to satisfy Eq. (14), meaning that the shear stress is equal in all veins irrespective of their thickness. This also suggests that the average velocity $\bar{v}$ is proportional to r_0 because $Q \propto \bar{v}r_0^2$. This relationshiop is supported by some studies of Takamatsu *et al.* [30, 31], where velocities increased linearly with width for tubes constrained in a narrow channels. Whilst the molecular mechanism underpinning current-reinforcement is not known yet, this observation leads to the interesting possibility that sensing an increase in wall shear above a fixed point provides a molecular trigger to changing vessel diameter. Thick bundles of actin filament are observed to co-align with each other at the interface between the vein wall and the flowing fluid along these emerging channels as they thicken to become veins [32]. Shear stress at the vein wall is a good candidate to align the F-actin bundles, in a similar manner to that reported for shear banding of F-actin in solution [33]. This would provide an intra-cellular analogy to the control of vessel development in blood vascular systems by shear forces.

It is less clear how the network forms from an initially homogeneous plasmodial sheet. It is known that actin-myosin interactions generate contractions in small plasmodial droplets that can become organised as propagating waves or spirals (e.g. [34]). This provides a driving force for protoplasmic streaming, although initially it is undirected and uniform across the plasmodium. However, Guy *et al.* proposed for a migrating plasmodium that an initially homogeneous flow of protoplasmic sol can de-stabilise the actin skeleton as it moves through the porous protoplasmic gel [35]. This in turn initiates channel formation if the flow is sufficiently rapid, through flow-dependent actin disruption and gel-sol interconversion. Such a process appears to operate rapidly in the newly formed plasmodium, as the emergent network spanning the entire arena is visible with a few hours, correctly oriented towards the exit, and remains stable until the arena is almost fully evacuated (Fig. 1).

From its inception, the network is able to drain all parts of the arena equally irrespective of the shape. From a biological perspective the plasmodium in the arena has no access to food, so it makes sense to re-deploy the biomass elsewhere as rapidly as possible. Equally, it is important that the exit does not becomes clogged nor

should the plasmodium become disconnected, prioritising an orderly evacuation sequence. In the case of *Physarum* this appears to emerge as a natural consequence of the current-reinforcement model that establishes a similar hydrodynamic conductivity from all peripheral parts of the network. This is in stark contrast to observations and models of human evacuation, where exit routes rapidly become jammed with rushing people, and further movement is restricted by the strong frictional force between trapped pedestrians [36], although exit rates can be improved by placing an obstacle off-center and just in front of the exit [37].

The current-reinforcement model generated networks similar to those found experimentally, although the kinetics leading to emergence of the network in the model differed, particularly in the early stages, where the initial conditions dominated behaviour of the simulation. For example, starting with uniform small radii and constant input current to find the initial flow in each vein also required extremely high pressures in the peripheral part of the arena, with consequential increases in friction energy and total volume (Fig. 9), until some tubes with larger diameter emerged. In addition, the simulation model did not predict the long-term evacuation dynamics as the current input rate to each node did not decrease as would be expected as the mass was evacuated.

The principles of current-reinforcement are well-established for a number of biological systems as diverse as ant trails and human trails [14]. The precise form of the model is context specific, but most models incorporate similar elements. For example, Hu and Cai [4] proposed a very similar model which is, in our notation, expressed as

$$\frac{\mathrm{d}D_{ij}}{\mathrm{d}t} = c\left(\frac{Q_{ij}^2}{D_{ij}^{\gamma+1}} - \tau_e^2\right) D_{ij}, \qquad (15)$$

where c, γ, and τ_e are constants. Furthermore, Haskovec *et al.* [38, 39] presented a system of partial differential equations that contained a current term effecting a time evolution of conductivity. While these models consider specific current effects, the model of Eq. (5) can take an arbitrary thickening factor $f(|Q_{ij}|)$. There is increasing interest in exploring the limits of behaviour for generic current-reinforcement dynamics and how these may play out on network topologies other than 2-D planar systems where they first emerged, where they show very rich behaviour (e.g., [40]).

In the evacuation experiment conducted here, the exit acts as a bottleneck that controls protoplasmic redeployment as all the biomass must pass through this point. As the rate of draining is homogeneous across the arena, the contribution of biomass from every local part of the plasmodial sheet to the bottleneck is equal. Nevertheless, on the timescale of minutes, shuttle streaming of protoplasm rapidly mixes the cytoplasm within the plasmodium [15], with biomass periodically transported both to the bottleneck and back to the periphery. Interestingly, this means that both biophysical changes, such as mechanical momentum of mass flow, and chemical components, such as nutrients or signalling molecules, may cycle between distal parts of the plasmodium and the bottleneck. This opens the possibility for information transfer of either physical or chemical signals to and from the bottleneck, which acts as a transient hub controlling intracellular communication through the vein network. Such organization of network structure may be required to coordinate behaviour in response to local information that could be sensed at any part of the plasmodium. In other words, all local regions are homogeneously inspected by the bottleneck at regular intervals. This implies that the plasmodium has the potential ability to organize an *ad hoc* functional center in response to varying external conditions.

Acknowledgments

This research was supported by grants from JSPS KAKENHI (26310202, TN), Grant-in-Aid for Scientific Research on Innovative Area from MEXT (25111726 and 25103006, TN), the Strategic Japanese-Swedish Research Cooperative Program, Japan Science and Technology Agency (JST, TN), The Human Frontier Science Program (RGP0053/2012, MDF), and the Leverhulme Foundation (RPG-2015-437, MDF).

[1] G. B. West, J. H. Brown and B. J. Enquist, "A general model for the origin of allometric scaling laws in biology", Science, **276**, 5309, pp. 122–126 (1997).

[2] J. R. Banavar, A. Maritan and A. Rinaldo, "Size and form in efficient transportation networks", Nature, **399**, 6732, pp. 130–132 (1999).

[3] P. S. Dodds, "Optimal form of branching supply and collection networks", Physical Review Letters, **104**, p. 048702 (2010).

[4] D. Hu and D. Cai, "Adaptation and optimization of biological transport networks", Physical Review Letters, **111**, p. 138701 (2013).

[5] F. Corson, "Fluctuations and redundancy in optimal transport networks", Phys. Rev. Lett., **104**, p. 048703 (2010).

[6] E. Katifori, G. J. Szöllősi and M. O. Magnasco, "Damage and fluctuations induce loops in optimal transport networks", Physical Review Letters, **104**, p. 048704 (2010).

[7] T. Nakagaki, H. Yamada and T. Ueda, "Interaction between cell shape and contraction pattern in the physarum plasmodium", Biophysical Chemistry, **84**, 3, pp. 195 – 204 (2000).

[8] A. Tero, R. Kobayashi and T. Nakagaki, "A mathematical model for adaptive transport network in path finding

by true slime mold", Journal of Theoretical Biology, **244**, 4, pp. 553 – 564 (2007).

[9] A. Tero, S. Takagi, T. Saigusa, K. Ito, D. P. Bebber, M. D. Fricker, K. Yumiki, R. Kobayashi and T. Nakagaki, "Rules for biologically inspired adaptive network design", Science, **327**, 5964, pp. 439–442 (2010).

[10] T. Nakagaki, M. Iima, T. Ueda, Y. Nishiura, T. Saigusa, A. Tero, R. Kobayashi and K. Showalter, "Minimum-risk path finding by an adaptive amoebal network", Physical Review Letters, **99**, p. 068104 (2007).

[11] T. Nakagaki, H. Yamada and Á. Tóth, "Intelligence: Maze-solving by an amoeboid organism", Nature, **407**, 6803, pp. 470–470 (2000).

[12] W. Baumgarten, T. Ueda and M. J. Hauser, "Plasmodial vein networks of the slime mold physarum polycephalum form regular graphs", Physical Review E, **82**, 4, p. 046113 (2010).

[13] A. Fessel, C. Oettmeier, E. Bernitt, N. C. Gauthier and H.-G. Döbereiner, "*Physarum polycephalum* percolation as a paradigm for topological phase transitions in transportation networks", Physical Review Letters, **109**, p. 078103 (2012).

[14] Q. Ma, A. Johansson, A. Tero, T. Nakagaki and D. J. T. Sumpter, "Current-reinforced random walks for constructing transport networks", Journal of The Royal Society Interface, **10**, 80 (2012).

[15] K. Alim, G. Amselem, F. Peaudecerf, M. P. Brenner and A. Pringle, "Random network peristalsis in physarum polycephalum organizes fluid flows across an individual", Proceedings of the National Academy of Sciences, **110**, 33, pp. 13306–13311 (2013).

[16] V. Teplov, Y. Romanovsky and O. Latushkin, "A continuum model of contraction waves and protoplasm streaming in strands of physarum plasmodium", Biosystems, **24**, 4, pp. 269 – 289 (1991).

[17] M. Radszuweit, H. Engel and M. Bär, "A model for oscillations and pattern formation in protoplasmic droplets of physarum polycephalum", The European Physical Journal Special Topics, **191**, 1, pp. 159–172 (2010).

[18] K.-i. Ueda, S. Takagi, Y. Nishiura and T. Nakagaki, "Mathematical model for contemplative amoeboid locomotion", Physical Review E, **83**, 2, p. 021916 (2011).

[19] M. Radszuweit, S. Alonso, H. Engel and M. Bär, "Intracellular mechanochemical waves in an active poroelastic model", Physical Review Letters, **110**, p. 138102 (2013).

[20] M. Radszuweit, H. Engel and M. Bär, "An active poroelastic model for mechanochemical patterns in protoplasmic droplets of *Physarum polycephalum*", PLoS ONE, **9**, 6, pp. 1–12 (2014).

[21] S. Alonso, U. Strachauer, M. Radszuweit, M. Bär and M. J. Hauser, "Oscillations and uniaxial mechanochemical waves in a model of an active poroelastic medium: Application to deformation patterns in protoplasmic droplets of physarum polycephalum", Physica D: Nonlinear Phenomena, **318-319**, pp. 58 – 69 (2016).

[22] O. L. Lewis, S. Zhang, R. D. Guy and J. C. del Álamo, "Coordination of contractility, adhesion and flow in migrating physarum amoebae", Journal of The Royal Society Interface, **12**, 106 (2015).

[23] C. D. Murray, "The physiological principle of minimum work applied to the angle of branching of arteries", The Journal of General Physiology, **9**, 6, pp. 835–841 (1926).

[24] T. F. Sherman, "On connecting large vessels to small. the meaning of murray's law.", The Journal of General Physiology, **78**, 4, pp. 431–453 (1981).

[25] C. A. Price, J. S. Weitz, V. M. Savage, J. Stegen, A. Clarke, D. A. Coomes, P. S. Dodds, R. S. Etienne, A. J. Kerkhoff, K. McCulloh, K. J. Niklas, H. Olff and N. G. Swenson, "Testing the metabolic theory of ecology", Ecology Letters, **15**, 12, pp. 1465–1474 (2012).

[26] M. G. Newberry, D. B. Ennis and V. M. Savage, "Testing foundations of biological scaling theory using automated measurements of vascular networks", PLoS Comput Biol, **11**, 8, pp. 1–18 (2015).

[27] N. Suwa, T. Niwa, H. Fukasawa and Y. Sasaki, "Estimation of intravascular blood pressure gradient by mathematical analysis of arterial casts", The Tohoku journal of experimental medicine, **79**, 2, pp. 168–198 (1963).

[28] A. Adamatzky and J. Jones, "Road planning with slime mould: If physarum built motorways it would route m6/m74 through newcastle", International Journal of Bifurcation and Chaos, **20**, 10, pp. 3065–3084 (2010).

[29] A. Adamatzky, "Route 20, autobahn 7, and slime mold: approximating the longest roads in usa and germany with slime mold on 3-d terrains", Cybernetics, IEEE Transactions on, **44**, 1, pp. 126–136 (2014).

[30] A. Takamatsu and T. Fujii, "Construction of a living coupled oscillator system of plasmodial slime mold by a microfabricated structure", Sensors Update, **10**, 1, pp. 33–46 (2002).

[31] A. Takamatsu, T. Fujii, and I. Endo, "Control of interaction strength in a network of the true slime mold by a microfabricated structure", Biosystems, **55**, 1–3, pp. 33–38 (2000).

[32] W. Stockem and K. Brix, "Analysis of microfilament organization and contractile activities in physarum", Vol. 149 of International Review of Cytology, Academic Press, pp. 145 – 215 (1994).

[33] I. Kunita, K. Sato, Y. Tanaka, Y. Takikawa, H. Orihara and T. Nakagaki, "Shear banding in an f-actin solution", Physical Review Letters, **109**, p. 248303 (2012).

[34] M. Fricker, M. Tlalka, D. Bebber, S. Tagaki, S. Watkinson and P. Darrah, "Fourier-based spatial mapping of oscillatory phenomena in fungi", Fungal Genetics and Biology, **44**, 11, pp. 1077 – 1084 (2007).

[35] R. D. Guy, T. Nakagaki and G. B. Wright, "Flow-induced channel formation in the cytoplasm of motile cells", Physical Review E, **84**, p. 016310 (2011).

[36] D. Helbing, I. Farkas and T. Vicsek, "Simulating dynamical features of escape panic", Nature, **407**, 6803, pp. 487–490 (2000).

[37] A. Kirchner, K. Nishinari and A. Schadschneider, "Friction effects and clogging in a cellular automaton model for pedestrian dynamics", Physical Review E, **67**, p. 056122 (2003).

[38] J. Haskovec, P. Markowich and B. Perthame, "Mathematical analysis of a pde system for biological network formation", Communications in Partial Differential Equations, **40**, 5, pp. 918–956 (2015).

[39] J. Haskovec, P. Markowich, B. Perthame and M. Schlottbom, "Notes on a pde system for biological network formation", Nonlinear Analysis: Theory, Methods & Applications, **138**, pp. 127 – 155 (2016).

[40] J. Gräwer, C. D. Modes, M. O. Magnasco and E. Katifori, "Structural self-assembly and avalanchelike dynamics in locally adaptive networks", Physical Review E, **92**, p. 012801 (2015).